

Modeling kinetic effects of charged vacancies on electromechanical responses of ferroelectrics: Rayleighian approach

Rajeev Kumar , * Shuaifang Zhang , and P. Ganesh †

Center for Nanophase Materials Sciences, Oak Ridge National Laboratory, Oak Ridge, Tennessee 37831, USA



(Received 24 March 2024; accepted 19 November 2024; published 15 January 2025)

Understanding the time-dependent effects of charged vacancies on the electromechanical responses of materials is at the forefront of research for designing materials exhibiting metal-insulator transitions and memristive behavior. A Rayleighian approach is used to develop a model for studying the nonlinear kinetics of the reaction leading to generation of vacancies and electrons via the dissociation of vacancy-electron pairs. Also, diffusion and elastic effects of charged vacancies are considered to model polarization-electric potential and strain-electric potential hysteresis loops. The model captures multiphysics phenomena by introducing couplings among polarization, the electric potential, stress, strain, and concentrations of charged (multivalent) vacancies and electrons (treated as classical negatively charged particles), where the concentrations can vary due to association-dissociation reactions. A derivation of coupled time-dependent equations based on the Rayleighian approach is presented. Three limiting cases of the governing equations are considered, highlighting the effects of (1) nonlinear reaction kinetics on the generation of charged vacancies and electrons, (2) Vegard's law (i.e., the concentration-dependent local strain) on asymmetric strain-electric potential relations, and (3) coupling between a fast component and the slow component of the net polarization on the polarization-electric-field relations. The Rayleighian approach discussed in this work should pave the way for developing a multiscale modeling framework in a thermodynamically consistent manner while capturing multiphysics phenomena in ferroelectric materials.

DOI: 10.1103/PhysRevResearch.7.013059

I. INTRODUCTION

Fundamental principles, which can help in the design of materials exhibiting a metal-insulator transition [1] and memory effects, are under extensive scrutiny by a number of researchers in the fields of spintronics [2], ferroelectrics [3], and neuromorphic computing [4]. Experimental discoveries [5] connecting oxygen vacancies to unconventional ferroelectricity in films and metal-insulator transitions have led to research activities focused on understanding the effects of the vacancies on material properties. These activities include experimental measurements, which can decouple contributions to switching polarization from polar crystal phases and vacancy migration under applied electric fields, the transient effects of vacancy ordering [6], and the electrochemical effects due to surfaces [7]. In parallel, models capturing the effects of oxygen vacancies at different levels of approximation have been developed, including molecular models based on density functional theory [6], reactive force fields [8], and continuum models [9] capturing long-wavelength

physics. These research activities, experimental and theoretical, have unequivocally established that electrostatic effects due to vacancies are of paramount importance in controlling the properties of materials at length scales and timescales relevant to the application of materials in microelectronics. For example, Lin *et al.* [10] proposed a hypothesis that enhanced remnant polarization of a composite containing ferroelectric barium titanate (BaTiO_3) and a metallic nonferroelectric oxide of SrRuO_3 may be attributed to the accumulation of oxygen vacancies at the $\text{BaTiO}_3/\text{SrRuO}_3$ interface. Similarly, thin films (~ 80 nm) of BaTiO_3 grown on $\text{SrRuO}_3/\text{SrTiO}_3$ were studied recently [6] to understand the effects of oxygen vacancy injection on the electromechanical responses of the films. It has been established [6] that enhanced electromechanical responses in these films can be sustained by the injection of oxygen vacancies, and the kinetic effects due to the vacancies were postulated to be responsible for the responses.

Modeling kinetic effects due to vacancies in thin films of ferroelectric materials requires the use of a simulation method, which can capture the effects of multiple phases (varying in polarization and crystal symmetry) and multiphysics phenomena due to couplings among polarization, the electrostatic potential, strain, and vacancies. For long length scales and timescales, the phase field method has been used to model ferroelectric [11–13] materials using parameters which can be either inferred from experimental data or estimated using density functional theory (DFT). The phase field method has been used to model phenomena occurring at long timescales (of the order of seconds), such as domain wall motion [11]

*Contact author: kumarr@ornl.gov

†Contact author: ganeshp@ornl.gov

and domain nucleation [12]. This method incorporates a thermodynamic free energy similar to that originally proposed by Landau, Ginzburg, and Devonshire for ferroelectricity in the bulk (i.e., without surfaces), generalized to inhomogeneous systems and the time domain. The free energy is typically written in terms of a space- and time-dependent polarization vector and its gradients. The coefficients of various terms in the free energy can be either kept phenomenological or estimated from first-principles calculations such as DFT after identifying the underlying origins of polarization in terms of atomic displacements. For example, the free energies of some ferroelectrics materials were summarized by Chen [14].

In the last two decades, a number of phase field models were developed to understand the effects of vacancies in ferroelectric materials. For example, Zhang *et al.* [15] developed a phase field model for ferroelectrics with oxygen vacancies by treating them as defect dipoles and investigated the oxygen-vacancy-induced memory effect and large recoverable strain in BaTiO₃. Cao *et al.* [16] treated the vacancies as charged defects and developed a phase field method for BaTiO₃ by coupling time-dependent equations for polarization with the Poisson-Nernst-Planck equations for density of charges. Shindo *et al.* [17] used a phase field model to study the electromechanical response of polycrystalline BaTiO₃ with oxygen vacancies by treating the vacancies as defect dipoles. Recently, Fedeli *et al.* [18] presented a phase field model for ferroelectrics by treating defects in the single crystal and polycrystal structures as voids, charged point defects, and polarization pinned objects, such that the polarization pinned objects retained their polarization during the cycling of electric field. Last, Kelley *et al.* [6] proposed a new free energy by including the impact of oxygen vacancies on not only polarization but also strains, which they used to understand the asymmetry in the polarization-electrostatic potential ($P - \psi$) loops with different concentrations of oxygen vacancies. In order to simplify the semianalytical analysis, they invoked an assumption that the vacancies move much faster than the polarization so that a steady-state approximation for relaxation of the densities of the vacancies can be justified. Despite these modeling efforts spanning two decades related to the modeling of vacancies and ferroelectrics, a unified theoretical framework which can be used to construct thermodynamically consistent kinetic models for thin films of ferroelectric materials with vacancies is still lacking. The development of such a theoretical framework is the main goal of this paper. Limiting cases are discussed to highlight the key features of this framework.

In this paper, a Rayleighian approach is used to develop time- and space-dependent equations for polarization; the densities of vacancies, electrons, and their pairs; the electrostatic potential; and strains. The approach has its basis in principles of linear irreversible thermodynamics and ensures that the second law of thermodynamics is obeyed. Numerical solutions of the coupled set of equations will be presented in a future work for the purpose of constructing average polarization-electric potential and strain-electric potential hysteresis loops. This paper is organized as follows: the details of the energy functional, the Rayleighian approach, and the coupled equations are presented in Sec. II. Different limits of the coupled set of equations are analyzed in Sec. III. Conclusions are presented in Sec. IV.

II. MODEL BUILDING FOR THIN FILMS OF FERROELECTRICS USING THE RAYLEIGHIAN APPROACH

A set of time-dependent equations can be derived to simulate ferroelectric materials like BaTiO₃ with vacancies. These equations can be derived using the principles of irreversible thermodynamics. For the derivation, we decompose local polarization into fast and slow components resulting from electronic and atomic/orientational motions, respectively. The fast component of the polarization $\mathbf{P}_e(\mathbf{r}, t)$ at a location \mathbf{r} at time t is assumed to be in equilibrium with the electric field $\mathbf{E}(\mathbf{r}, t) = -\nabla\psi(\mathbf{r}, t)$, i.e., $\mathbf{P}_e(\mathbf{r}, t) = \epsilon_0\epsilon_\infty\mathbf{E}(\mathbf{r}, t)$, where ϵ_0 is the permittivity of vacuum, ϵ_∞ is the infinite-frequency dielectric constant of the material, and ψ is the electrostatic potential. In contrast, the slow component $\mathbf{P}(\mathbf{r}, t)$ can be out of equilibrium, and time-dependent equations are derived for this component. Such a decomposition of the polarization is similar to the work by Marcus [19] focused on electron transfer processes. Coupling the slow component of polarization with the fast component is considered by introducing lattice strain. Diffusion of charged vacancies and electrons is considered by using their local densities as additional order parameters and following our previous work related to ion transport in polymerized ionic liquids [20]. Furthermore, reaction kinetics leading to electrochemical effects, which result from charge generation and the recombination of positively charged vacancies with electrons, are considered. The strain and concentration of the vacancies are coupled by Vegard's law [21], which is an empirical rule leading to a linear relation between the strain and the concentration of the vacancies. The mathematical framework leading to the equations, which can introduce couplings among the polarization, strain, diffusion, and reaction kinetics, is presented below.

Any material perturbed from equilibrium by the application of a small external force will try to approach equilibrium through various dissipative processes. Dissipative processes and the path must lead to a positive rate of entropy production per the second law of thermodynamics [20,22,23]. These statements were cast into a rigorous mathematical framework by Onsager [22] after he defined a functional called the Rayleighian, which consists of the rate of change of "free" energy (or entropy for isothermal processes) and a dissipation function. According to Onsager's variational principle, the most probable dynamics of a system is one that demonstrates the least dissipation. Linear relations among various fluxes and forces can hence be derived by minimizing the Rayleighian with respect to the velocities leading to the maximum rate of entropy production, and the resulting equations define the most probable path toward equilibrium [24,25]. The details of this so-called Onsager variational principle are presented elsewhere [22,24–26]. The construction of the Rayleighian requires the identification of independent fluxes, reaction rates, and constraints, which are discussed in the next section.

A. Independent fluxes, rates, and constraints

A model for understanding the effects of vacancies can be developed by using the principles of irreversible thermodynamics [20,22,23]. In particular, we use Onsager's variational

principle [26] to derive a set of equations for the polarization $\mathbf{P}(\mathbf{r}, t)$, strain tensor $\boldsymbol{\epsilon}(\mathbf{r}, t)$, and the number densities of electroactive vacancies [$\rho_+(\mathbf{r}, t)$], electrons [$\rho_-(\mathbf{r}, t)$], and their pairs [$\rho_\pm(\mathbf{r}, t)$], which are coupled via the electric field $\mathbf{E}(\mathbf{r}, t)$. The number densities $\rho_+(\mathbf{r}, t)$, $\rho_-(\mathbf{r}, t)$, and $\rho_\pm(\mathbf{r}, t)$ are assumed to satisfy

$$\frac{\partial \rho_i(\mathbf{r}, t)}{\partial t} = -\nabla \cdot \mathbf{j}_i(\mathbf{r}, t) + S_i(\mathbf{r}, t), \quad i = +, -, \pm, \quad (1)$$

where $\mathbf{j}_i(\mathbf{r}, t) = \rho_i(\mathbf{r}, t)\mathbf{v}_i(\mathbf{r}, t)$ is the diffusive flux, with $\mathbf{v}_i(\mathbf{r}, t)$ being the collective velocity of $i = +, -, \pm$. In Eq. (1), $S_i(\mathbf{r}, t)$ is the rate of change of the number density of i resulting from the dissociation and the formation of vacancy-electron pairs. We assume that the number densities satisfy the no-void condition at all locations at all times so that the sum of the volume fractions defined as $\phi_i(\mathbf{r}, t) = \rho_i(\mathbf{r}, t)/\rho_{io}$ is unity, i.e.,

$$\sum_{i=+,-,\pm} \phi_i(\mathbf{r}, t) = 1, \quad (2)$$

where $1/\rho_{io}$ is the molar volume of i . Using Eqs. (1) and (2), a constraint on the fluxes and the reaction rates is obtained, which is written as

$$\sum_{i=+,-,\pm} \left[-\nabla \cdot \left\{ \frac{\mathbf{j}_i(\mathbf{r}, t)}{\rho_{io}} \right\} + \frac{S_i(\mathbf{r}, t)}{\rho_{io}} \right] = 0 \quad (3)$$

Now, we need to construct relations between $\mathbf{j}_i(\mathbf{r}, t)$, $S_i(\mathbf{r}, t)$, and thermodynamic forces. In the following, we accomplish this by considering a functional called the Rayleighian R . Before defining the Rayleighian, we need to identify relevant independent fluxes \mathbf{j}_i , rates S_i , and thermodynamic forces.

To identify independent fluxes \mathbf{j}_i , rates S_i , and other constraints, we consider the rate of change of the total number $M(t)$ of particles in the vacancies, the electrons, and the pairs, defined as $M(t) = \int d\mathbf{r} [\rho_+(\mathbf{r}, t) + \rho_-(\mathbf{r}, t) + (z_+ + 1)\rho_\pm(\mathbf{r}, t)]$. Due to the fixed number of particles at all times, the rate of change of $M(t)$ must be zero, and the rate is given by

$$\begin{aligned} \frac{dM(t)}{dt} &= \int d\mathbf{r} [-\nabla \cdot \{\mathbf{j}_+(\mathbf{r}, t) + \mathbf{j}_-(\mathbf{r}, t) + (z_+ + 1)\mathbf{j}_\pm(\mathbf{r}, t)\} \\ &\quad + \{S_+(\mathbf{r}, t) + S_-(\mathbf{r}, t) + (z_+ + 1)S_\pm(\mathbf{r}, t)\}] \\ &= \int d\Gamma \hat{\mathbf{n}} \cdot \{\mathbf{j}_+(\mathbf{r}, t) + \mathbf{j}_-(\mathbf{r}, t) + (z_+ + 1)\mathbf{j}_\pm(\mathbf{r}, t)\}, \end{aligned} \quad (4)$$

where we have used Eq. (1) and assumed $S_+(\mathbf{r}, t) + S_-(\mathbf{r}, t) + (z_+ + 1)S_\pm(\mathbf{r}, t) = 0$ so that the total number of particles remains the same due to the dissociation-association reactions. Here, Γ represents the surface enclosing the volume under consideration, $\hat{\mathbf{n}}$ is an outward normal at the surface, and we have used the divergence theorem. Now, equating $dM(t)/dt = 0$, Eq. (4) is satisfied if

$$\hat{\mathbf{n}} \cdot \{\mathbf{j}_+(\mathbf{r}, t) + \mathbf{j}_-(\mathbf{r}, t) + (z_+ + 1)\mathbf{j}_\pm(\mathbf{r}, t)\} = 0 \quad (5)$$

at the surface. Another constraint for the boundary fluxes is obtained by considering the rate of change of the total charge $C(t)$ of the vacancies and the electrons, defined as $C(t) = e \int d\mathbf{r} [z_+\rho_+(\mathbf{r}, t) - \rho_-(\mathbf{r}, t)]$, which must be zero due to the global electroneutrality at all times. The rate of change

of $C(t)$ is given by

$$\begin{aligned} \frac{dC(t)}{dt} &= e \int d\mathbf{r} [-\nabla \cdot \{z_+\mathbf{j}_+(\mathbf{r}, t) - \mathbf{j}_-(\mathbf{r}, t)\} \\ &\quad + \{z_+S_+(\mathbf{r}, t) - S_-(\mathbf{r}, t)\}] \\ &= \int d\Gamma \hat{\mathbf{n}} \cdot \{z_+\mathbf{j}_+(\mathbf{r}, t) - \mathbf{j}_-(\mathbf{r}, t)\} = 0, \end{aligned} \quad (6)$$

where we have assumed that $z_+S_+(\mathbf{r}, t) - S_-(\mathbf{r}, t) = 0$, i.e., the rate of charge generation due to the dissociation-association reactions is taken to be zero. Combining $S_+(\mathbf{r}, t) + S_-(\mathbf{r}, t) + (z_+ + 1)S_\pm(\mathbf{r}, t) = 0$ with $z_+S_+(\mathbf{r}, t) - S_-(\mathbf{r}, t) = 0$ leads to

$$S_+(\mathbf{r}, t) = \frac{1}{z_+} S_-(\mathbf{r}, t) = -S_\pm(\mathbf{r}, t) \equiv -S(\mathbf{r}, t) \quad (7)$$

for the association-dissociation reactions involving electroneutral vacancy-electron pairs, positively charged vacancies with charge z_+e (where e is the charge of an electron), and neutralizing electrons. For example, $z_+ = 2$ in the case of oxygen vacancies. Equation (7) implies that there is only one independent reaction rate, which is taken to be $S(\mathbf{r}, t)$. Now, Eqs. (3) and (7) imply that there are only two independent fluxes out of the three fluxes \mathbf{j}_i . Based on a molecular description of the diffusion resulting from frictional forces and the relative motion of molecules, we work with the relative fluxes defined as $\hat{\mathbf{j}}_i(\mathbf{r}, t) = \phi_i(\mathbf{r}, t)[\mathbf{v}_i(\mathbf{r}, t) - \mathbf{v}(\mathbf{r}, t)]$, where

$$\mathbf{v}(\mathbf{r}, t) = \sum_{i=+,-,\pm} \phi_i(\mathbf{r}, t) \mathbf{v}_i(\mathbf{r}, t). \quad (8)$$

These relative fluxes are related by the relation

$$\sum_{i=+,-,\pm} \hat{\mathbf{j}}_i(\mathbf{r}, t) = 0, \quad (9)$$

and the Rayleighian can be written in terms of any two relative fluxes. Here, we choose $\hat{\mathbf{j}}_+$ and $\hat{\mathbf{j}}_-$ to study the effects of diffusion of the vacancies and the electrons, respectively. Equation (1) is rewritten in terms of these independent fluxes and rates in the form

$$\begin{aligned} \frac{\partial \phi_k(\mathbf{r}, t)}{\partial t} &= -\nabla \cdot \hat{\mathbf{j}}_k(\mathbf{r}, t) + \frac{1}{\rho_{ko}} S_k(\mathbf{r}, t) - \nabla \cdot [\phi_k(\mathbf{r}, t) \mathbf{v}(\mathbf{r}, t)], \\ k &= +, -, \end{aligned} \quad (10)$$

and Eq. (3) can be written as

$$\nabla \cdot \mathbf{v}(\mathbf{r}, t) + S(\mathbf{r}, t) \left\{ \frac{1}{\rho_{+o}} + \frac{z_+}{\rho_{-o}} - \frac{1}{\rho_{\pm o}} \right\} = 0. \quad (11)$$

Equations (5) and (6) are rewritten in terms of $\hat{\mathbf{j}}_{i=+,-,\pm} \cdot \hat{\mathbf{n}}$ as

$$\begin{aligned} &\hat{\mathbf{n}} \cdot \{\rho_{+o}\hat{\mathbf{j}}_+(\mathbf{r}, t) + \rho_{-o}\hat{\mathbf{j}}_-(\mathbf{r}, t) + (z_+ + 1)\rho_{\pm o}\hat{\mathbf{j}}_\pm(\mathbf{r}, t)\} \\ &+ \hat{\mathbf{n}} \cdot \{[\rho_{+o}\phi_+(\mathbf{r}, t) + \rho_{-o}\phi_-(\mathbf{r}, t) \\ &+ (z_+ + 1)\rho_{\pm o}\phi_\pm(\mathbf{r}, t)]\mathbf{v}(\mathbf{r}, t)\} = 0, \end{aligned} \quad (12)$$

$$\begin{aligned} &\hat{\mathbf{n}} \cdot \{z_+\rho_{+o}\hat{\mathbf{j}}_+(\mathbf{r}, t) - \rho_{-o}\hat{\mathbf{j}}_-(\mathbf{r}, t) \\ &+ [z_+\rho_{+o}\phi_+(\mathbf{r}, t) - \rho_{-o}\phi_-(\mathbf{r}, t)]\mathbf{v}(\mathbf{r}, t)\} = 0. \end{aligned} \quad (13)$$

These equations show that there are two boundary fluxes, which are independent. They are chosen to be $\hat{\mathbf{j}}_{k=+,-} \cdot \hat{\mathbf{n}}$. In summary, independent fluxes and rates are $\hat{\mathbf{j}}_{k=+,-}$, $\hat{\mathbf{j}}_{k=+,-} \cdot \hat{\mathbf{n}}$ and S , respectively. In addition, we need to consider the constraint written as Eq. (11) and discussed above.

B. Rayleighian

To apply Onsager's variational principle, a Rayleighian $R(t)$ for the thin films of ferroelectric materials can be defined as [20,27]

$$R(t) = \frac{dH(t)}{dt} + W(t) - \int d\mathbf{r} p(\mathbf{r}, t) \left[\nabla \cdot \mathbf{v}(\mathbf{r}, t) + S(\mathbf{r}, t) \left\{ \frac{1}{\rho_{+o}} + \frac{z_+}{\rho_{-o}} - \frac{1}{\rho_{\pm o}} \right\} \right], \quad (14)$$

where $H(t)$ is the time-dependent energy functional (presented in the next section), $p(\mathbf{r}, t)$ is Lagrange's multiplier to enforce the constraint [see Eq. (11)], and W is the dissipation function. We should point out that the functional form

$$\begin{aligned} W(t) = & \frac{\tau_p}{2} \int d\mathbf{r} \left[\frac{\partial \mathbf{P}(\mathbf{r}, t)}{\partial t} + [\mathbf{v}_l(\mathbf{r}, t) \cdot \nabla] \mathbf{P}(\mathbf{r}, t) + \frac{1}{2} \mathbf{P}(\mathbf{r}, t) \times [\nabla \times \mathbf{v}_l(\mathbf{r}, t)] \right]^2 \\ & + \frac{1}{2} \int d\mathbf{r} \sum_{k=+, -} \sum_{k'=+, -} L_{kk'}(\mathbf{r}, t) \rho_{ko} \rho_{k'o} \hat{\mathbf{j}}_k(\mathbf{r}, t) \cdot \hat{\mathbf{j}}_{k'}(\mathbf{r}, t) \\ & + \frac{1}{2} \int d\mathbf{r} \sum_{k=+, -} \sum_{k'=+, -} M_{kk'}(\mathbf{r}, t) \rho_{ko} \rho_{k'o} [\hat{\mathbf{j}}_k(\mathbf{r}, t) \cdot \hat{\mathbf{n}}] [\hat{\mathbf{j}}_{k'}(\mathbf{r}, t) \cdot \hat{\mathbf{n}}] \\ & + \frac{1}{2} \int d\mathbf{r} \omega(\mathbf{r}, t) S^2(\mathbf{r}, t). \end{aligned} \quad (15)$$

Here, τ_p and $L_{kk'}$ are parameters characterizing the timescale for change in polarization \mathbf{P} and the friction coefficient for the motion of the vacancies and electrons relative to $\mathbf{v}(\mathbf{r}, t)$ [defined by Eq. (8)]. Similarly, $M_{kk'}$ are the parameters characterizing the dissipation due to the relative fluxes at the boundaries. Also, $\mathbf{v}_l(\mathbf{r}, t) = \sum_{l=1,2,3} [\frac{\partial u_l(\mathbf{r}, t)}{\partial t}] \hat{\mathbf{i}}_l$ is the net velocity of an underlying lattice, where $\hat{\mathbf{i}}_l$ are unit vectors and $u_l(\mathbf{r}, t)$ is the displacement of underlying atoms at location \mathbf{r} at time t . In general, $L_{kk'}$ and $M_{kk'}$ can be concentration dependent, but each matrix with either $L_{kk'}$ or $M_{kk'}$ as its elements must be positive definite for the positive entropy production. The last term in Eq. (15) is the dissipation due to the reaction with a prefactor ω , which is related to the rate of vacancy-electron pair dissociation and recombination.

In the following, we present an explicit expression for $H(t)$ by using thermodynamic free energy and by generalizing it after considering additional effects of the charged vacancies.

C. Energy functional

To derive a set of time-dependent equations, we use an energy functional, written as

$$\begin{aligned} H(t) = & \int d\mathbf{r} [H_{\text{LGD}}\{\mathbf{P}\} + H_{\text{grad}}\{\nabla \mathbf{P}\} + H_{\text{mech}}\{\mathbf{P}, \boldsymbol{\epsilon}, \rho_+\} \\ & + H_{\text{self}}\{\rho_+, \rho_-, \rho_\pm\} + H_{\text{elec}}\{\mathbf{P}, \mathbf{E} = -\nabla \psi, \rho_+, \rho_-\} \\ & + H_{\text{mix}}\{\rho_+, \rho_-, \rho_\pm, \nabla \rho_+, \nabla \rho_-, \nabla \rho_\pm\}] \end{aligned} \quad (16)$$

$$\equiv \int d\mathbf{r} h\{\mathbf{P}, \nabla \mathbf{P}, \rho_+, \rho_-, \rho_\pm, \nabla \rho_+, \nabla \rho_-, \nabla \rho_\pm, \mathbf{E}, \boldsymbol{\epsilon}\}, \quad (17)$$

of the dissipation function is assumed to be known in order to use the variational principle and there is no prescription for deriving it. In this paper, we present a functional form for the dissipation function by including various multiphysics phenomena and ensuring that the derived equations lead to known relations in various limiting cases. For example, W has contributions from the coupling of the polarization with the lattice velocity, derived by Hubbard and Onsager [28] using the approximation of fast rotational relaxation [23,29]. Also, contributions from friction, which result from the relative motions of charged vacancies and electrons with respect to the velocity $\mathbf{v}(\mathbf{r}, t)$ [see Eq. (8)], are included [20,26]. With the addition of these contributions, W can be written as

where H_{LGD} is the Landau-Ginzburg-Devonshire (LGD) energy density [3], written in terms of time-dependent polarization by invoking local-equilibrium approximation [23]. Similarly, H_{grad} is the gradient/interfacial energy density capturing the effects of inhomogeneous polarization in the long-wavelength limit. Explicit expressions for these contributions are presented in Appendix A for BaTiO₃ in the seminal work by Chen and coworkers [14]. Coupling between the polarization and the strain is encoded in H_{mech} , which is the mechanical strain energy density, where $\boldsymbol{\epsilon}$ is the strain tensor. Considering the limit of low deformation, the mechanical strain energy density [30] can be defined as

$$\begin{aligned} H_{\text{mech}} = & \frac{1}{2} \boldsymbol{\sigma}(\mathbf{r}, t) : [\boldsymbol{\epsilon}(\mathbf{r}, t) - \boldsymbol{\epsilon}^0(\mathbf{r}, t)] \\ & \equiv \frac{C_{ijkl}}{2} [\varepsilon_{ij}(\mathbf{r}, t) - \varepsilon_{ij}^0(\mathbf{r}, t)] [\varepsilon_{kl}(\mathbf{r}, t) - \varepsilon_{kl}^0(\mathbf{r}, t)], \end{aligned} \quad (18)$$

where $\varepsilon_{ij}(\mathbf{r}, t) = [\partial u_i / \partial x_j + \partial u_j / \partial x_i]/2$ is the ij element of the total lattice-strain tensor [31], with x_i being i th component of the spatial vector \mathbf{r} and $u_i(\mathbf{r}, t)$ being the i th component of the displacement vector of lattice; $\boldsymbol{\sigma}$ is the stress tensor; and C_{ijkl} is the rank 4 elasticity tensor. Ferroelectric materials can have spontaneous strain even in stress-free conditions, and such a strain tensor (eigenstrain [31]) is denoted as ε_{ij}^0 , results from electrostriction and Vegard effects, and can be defined as [6,14,32],

$$\varepsilon_{ij}^0(\mathbf{r}, t) = Q_{ijkl} P_k(\mathbf{r}, t) P_l(\mathbf{r}, t) + w_{ij}^v \rho_+(\mathbf{r}, t), \quad (19)$$

where Q_{ijkl} is a rank 4 order tensor. In this notation, $\varepsilon_{ij}(\mathbf{r}, t)$ is the tensor containing both elastic and eigenstrain components of the strain. Furthermore, the effects of the vacancies on the

strain are included in the last term in Eq. (19), where w_{ij}^v are phenomenological parameters. Here, Einstein's notation of a sum over repeated indices is used.

H_{self} is the self-energy density for creating the vacancies, electrons, and their pairs, written as

$$H_{\text{self}} = \sum_{i=+,-,\pm} G_{io} \rho_i(\mathbf{r}, t), \quad (20)$$

where G_{io} is the self-energy [33] for creating i . H_{elec} is the excess electrical energy density, written as [19]

$$H_{\text{elec}} = [z_+ \rho_+(\mathbf{r}, t) - \rho_-(\mathbf{r}, t)] e \psi(\mathbf{r}, t) - \frac{\epsilon_0 \epsilon_\infty}{2} \mathbf{E}^2(\mathbf{r}, t) - [\mathbf{P}(\mathbf{r}, t) \cdot \mathbf{E}(\mathbf{r}, t)], \quad (21)$$

where $\mathbf{E}(\mathbf{r}, t) = -\nabla \psi(\mathbf{r}, t)$ is the electric field and ψ is the electrostatic potential. z_+ is the valency of the oxygen vacancy, and e is the charge of an electron. Here, the pairs of the vacancies and the electrons are assumed to carry no charge. Furthermore, $-\frac{\delta[\int d\mathbf{r} H_{\text{elec}}]}{\delta \mathbf{E}(\mathbf{r}', t)} = \mathbf{D}(\mathbf{r}', t) = \epsilon_0 \epsilon_\infty \mathbf{E}(\mathbf{r}', t) + \mathbf{P}(\mathbf{r}', t)$ can be readily identified as the dielectric displacement vector.

Excess entropy of mixing vacancies, electrons, and their pairs is defined as H_{mix} along with the entropic cost of generating their inhomogeneous density profiles, written as [20]

$$H_{\text{mix}} = k_B T \sum_{i=+,-,\pm} \left\{ \rho_i(\mathbf{r}, t) \ln \left[\frac{\rho_i(\mathbf{r}, t)}{\rho_{io}} \right] + \frac{1}{2} \kappa_i |\nabla \rho_i(\mathbf{r}, t)|^2 \right\}. \quad (22)$$

The logarithmic terms in Eq. (22) can be derived by considering the number of ways in which the vacancies, the electrons, and the pairs can be distributed in space, such that their total number remain fixed. κ_i is the coefficient of the square-gradient term [34], which penalizes inhomogeneous density profiles of i .

With the dissipation and energy functional given by Eqs. (15) and (17), respectively, the Rayleighian has been specified [see Eq. (14)] completely, with quantities like τ_p , $L_{kk'}$, $M_{kk'}$, and ω taken as inputs. After the Rayleighian is constructed, a set of equations can be systematically derived by optimizing R with respect to $\frac{\partial \mathbf{P}(\mathbf{r}, t)}{\partial t}$, $\hat{\mathbf{j}}_{i=+,-}$, $\hat{\mathbf{j}}_{i=+,-} \cdot \hat{\mathbf{n}}$, S , and $\mathbf{v}_l(\mathbf{r}, t)$. The set is complemented by two additional equations: one for Lagrange's multiplier p and one for the electrostatic potential ψ . In total, nine coupled equations are derived in the next section.

D. Governing equations: Linear irreversible thermodynamics

We assume that the electrostatic potential adjusts itself so fast that the stationary condition $\frac{\delta H}{\delta \psi(\mathbf{r}, t)} = 0$ is satisfied at all times and at all locations. Explicitly, this leads to

$$\epsilon_0 \epsilon_\infty \nabla^2 \psi(\mathbf{r}, t) - \nabla \cdot \mathbf{P}(\mathbf{r}, t) + e[z_+ \rho_+(\mathbf{r}, t) - \rho_-(\mathbf{r}, t)] = 0, \quad (23)$$

or, equivalently,

$$\nabla \cdot \mathbf{D}(\mathbf{r}, t) = e[z_+ \rho_+(\mathbf{r}, t) - \rho_-(\mathbf{r}, t)], \quad (24)$$

where the right-hand side is the local charge density. Evaluating $\delta R(t)/\delta \{\frac{\partial \mathbf{P}(\mathbf{r}, t)}{\partial t}\} = 0$, we get the governing equations for

the three components of polarization P_1 , P_2 , and P_3 such that

$$\begin{aligned} \frac{\partial \mathbf{P}(\mathbf{r}, t)}{\partial t} + [\mathbf{v}_l(\mathbf{r}, t) \cdot \nabla] \mathbf{P}(\mathbf{r}, t) + \frac{1}{2} \mathbf{P}(\mathbf{r}, t) \times [\nabla \times \mathbf{v}_l(\mathbf{r}, t)] \\ = -\frac{1}{\tau_p} \frac{\delta [\int d\mathbf{r} h\{\mathbf{P}(\mathbf{r}', t)\}]}{\delta \mathbf{P}(\mathbf{r}, t)} \equiv \mathbf{P}^*(\mathbf{r}, t). \end{aligned} \quad (25)$$

The functional h is defined in Eq. (17), and its dependences on variables other than the polarization are suppressed here. Similarly, $\delta R(t)/\delta \mathbf{v}_l(\mathbf{r}, t) = 0$ leads to

$$\begin{aligned} \nabla \cdot \boldsymbol{\sigma}(\mathbf{r}, t) &= \frac{\tau_p}{2} \{ \nabla [\mathbf{P}^*(\mathbf{r}, t) \cdot \mathbf{P}(\mathbf{r}, t)] - \mathbf{P}(\mathbf{r}, t) \\ &\quad \times [\nabla \times \mathbf{P}^*(\mathbf{r}, t)] - \mathbf{P}^*(\mathbf{r}, t) \times [\nabla \times \mathbf{P}(\mathbf{r}, t)] \\ &\quad - \mathbf{P}(\mathbf{r}, t) [\nabla \cdot \mathbf{P}^*(\mathbf{r}, t)] + \mathbf{P}^*(\mathbf{r}, t) [\nabla \cdot \mathbf{P}(\mathbf{r}, t)] \}, \end{aligned} \quad (26)$$

where we have used $dH_{\text{mech}}/dt = \boldsymbol{\sigma}(\mathbf{r}, t) : [\nabla \mathbf{v}_l(\mathbf{r}, t) - \frac{\partial \epsilon_{ij}^0(\mathbf{r}, t)}{\partial t}]$. With the constitutive relation,

$$\sigma_{ij}(\mathbf{r}, t) = C_{ijkl} [\epsilon_{kl}(\mathbf{r}, t) - \epsilon_{kl}^0(\mathbf{r}, t)]. \quad (27)$$

Equation (26) can be used to study the effects of strains. We should point out that in general, $\sigma_{ij}(\mathbf{r}, t)$ should be computed from gradients of the lattice velocity. Here, we choose a simpler and intuitive linear constitutive relation [see Eq. (27)] between stress and strain. Optimizations of $R(t)$ with respect to $\hat{\mathbf{j}}_{k=+,-}$ and $\hat{\mathbf{j}}_{k=+,-} \cdot \hat{\mathbf{n}}$ give

$$\nabla [\mu_k(\mathbf{r}, t) - \mu_{\pm}(\mathbf{r}, t)] = - \sum_{k'=+,-} L_{kk'}(\mathbf{r}, t) \rho_{ko} \rho_{k'o} \hat{\mathbf{j}}_{k'}(\mathbf{r}, t) \cdot \hat{\mathbf{n}} \quad (28)$$

in the volume and

$$\mu_k(\mathbf{r}, t) - \mu_{\pm}(\mathbf{r}, t) = \sum_{k'=+,-} M_{kk'}(\mathbf{r}, t) \rho_{ko} \rho_{k'o} [\hat{\mathbf{j}}_{k'}(\mathbf{r}, t) \cdot \hat{\mathbf{n}}] \quad (29)$$

at the surface, respectively. Here, $\mu_k(\mathbf{r}, t) = \delta[\int d\mathbf{r} h\{\rho_k(\mathbf{r}', t)\}]/\delta \phi_k(\mathbf{r}, t)$ and becomes the local chemical potential of k in the steady state.

Evaluating $\delta R(t)/\delta S(\mathbf{r}, t) = 0$ gives

$$\begin{aligned} S(\mathbf{r}, t) &= \frac{1}{\omega(\mathbf{r}, t)} \left[\frac{\mu_+(\mathbf{r}, t)}{\rho_{+o}} + z_+ \frac{\mu_-(\mathbf{r}, t)}{\rho_{-o}} - \frac{\mu_{\pm}(\mathbf{r}, t)}{\rho_{\pm o}} \right. \\ &\quad \left. + p(\mathbf{r}, t) \left\{ \frac{1}{\rho_{+o}} + \frac{z_+}{\rho_{-o}} - \frac{1}{\rho_{\pm o}} \right\} \right]. \end{aligned} \quad (30)$$

Plugging the expression for S from Eq. (30) in Eq. (11), an equation for p is obtained, which closes this set of equations along with the boundary conditions shown in Eqs. (12) and (13).

E. Nonlinear reaction kinetics

Equation (30) shows that the reaction rate depends linearly on the chemical potentials, which limits the validity of the model presented here. We can improve this by introducing nonlinear relations between the reaction rate and the chemical potentials, similar to those forming the basis of Eyring's rate of reactions [35]. In this section, we present such a model, which could lead to nonlinear reaction kinetics like those in autocatalytic reactions [36]. For this purpose, we rewrite

Eq. (30) as a limiting case of the nonlinear relation,

$$S_{NL}(\mathbf{r}, t) = \frac{k_B T}{\omega(\mathbf{r}, t)} \left\{ \exp \left[\frac{\mu_+(\mathbf{r}, t) + p(\mathbf{r}, t)}{\rho_{+o} k_B T} \right] + z_+ \frac{\mu_-(\mathbf{r}, t) + p(\mathbf{r}, t)}{\rho_{-o} k_B T} \right\} - \exp \left[\frac{\mu_\pm(\mathbf{r}, t) + p(\mathbf{r}, t)}{\rho_{\pm o} k_B T} \right]. \quad (31)$$

Now, the Rayleighian $R \equiv R_{NL}$ based on S_{NL} can be constructed using Eq. (14), and it can be shown that

$$R_{NL}(t) = R(t) + \frac{1}{2} \int d\mathbf{r} \omega(\mathbf{r}, t) [S_{NL}(\mathbf{r}, t) - S(\mathbf{r}, t)]^2. \quad (32)$$

Note that $R(t) = -W(t) < 0$ per Onsager's variational principle, where the inequality is valid for a positive dissipation function and the governing equations derived in the last section. In contrast, $R_{NL}(t)$ can have either sign for $\omega(\mathbf{r}, t) > 0$. We should point out that $1/\omega(\mathbf{r}, t) = \exp[\frac{\mu^*(\mathbf{r}, t)}{\rho^{*o} k_B T}] \sim \rho^{*o} > 0$ is expected on the basis of Eyring's rate of reactions, where

$\mu^*(\mathbf{r}, t)$ and $1/\rho^{*o}$ are the chemical potential and volume of an activated complex [35], respectively. Physically, this relation between the prefactor $\omega(\mathbf{r}, t)$ and $\mu^*(\mathbf{r}, t)$ implies that the rate of reaction is linearly proportional to the concentration of the activated complexes [35]. More importantly, the probability of realizing a kinetic path with the nonlinear reaction rates is given by the Onsager-Machlup integral [24,25] based on the time integral of the difference $R_{NL}(t) - R(t)$. In particular, the probability of realizing the nonlinear reaction rates should be $\exp\{-\int_0^t dt' [R_{NL}(t') - R(t')] / 2k_B T\}$ per the theoretical works of Onsager and Machlup [24]. For this probability to be nonzero and significant enough, $\omega(\mathbf{r}, t)$ needs to be chosen in such a manner that the exponential of the negative of the Onsager-Machlup integral remains close to unity. In the following, we make such a choice for $\omega(\mathbf{r}, t)$ and keep all of the governing equations the same, except we replace S by S_{NL} to capture the effects of nonlinear reaction kinetics in the model for the ferroelectrics developed here.

Now, using Eqs. (10) and (28) and replacing S with S_{NL} [see Eq. (31)],

$$\frac{\partial \phi_+(\mathbf{r}, t)}{\partial t} = \nabla \cdot \left[\sum_{k'=+, -} \tilde{L}_{+k'}^{-1}(\mathbf{r}, t) \nabla [\mu_{k'}(\mathbf{r}, t) - \mu_\pm(\mathbf{r}, t)] \right] - \frac{1}{\rho_{+o}} S_{NL}(\mathbf{r}, t) - \nabla \cdot [\phi_+(\mathbf{r}, t) \mathbf{v}(\mathbf{r}, t)], \quad (33)$$

$$\frac{\partial \phi_-(\mathbf{r}, t)}{\partial t} = \nabla \cdot \left[\sum_{k'=+, -} \tilde{L}_{-k'}^{-1}(\mathbf{r}, t) \nabla [\mu_{k'}(\mathbf{r}, t) - \mu_\pm(\mathbf{r}, t)] \right] - \frac{z_+}{\rho_{-o}} S_{NL}(\mathbf{r}, t) - \nabla \cdot [\phi_-(\mathbf{r}, t) \mathbf{v}(\mathbf{r}, t)], \quad (34)$$

where $\tilde{L}_{kk'}^{-1}$ is the kk' element of the inverse matrix of $L_{kk'} \rho_{ko} \rho_{k'o}$. Three independent elements $\tilde{L}_{kk'}^{-1}$ can be interpreted [37] in terms of the ionic conductivity, transference number of the vacancies related to their partial ionic currents, and diffusion constants of the vacancy-electron pairs.

III. RESULTS

Here, we present an analysis of some limiting cases to highlight the key effects of the vacancies and aspects of the model. Numerical results obtained by solving the coupled equations will be presented in a separate publication. In the model presented here, we can capture the nonlinear effects of barriers on reaction rates and study the characteristic time for reactions. In the following, we consider three limiting cases: (1) a reaction-dominated regime leading to identification of a characteristic time, (2) a steady-state analysis highlighting coupling between the strain, electric potential, and vacancies, and (3) a vacancy-free regime, where coupling between the fast and slow components of the polarization can lead to effects of geometry manifesting in the stabilization of new topological configurations.

A. Reaction-dominated regime: Characteristic time

We consider a limiting case where vacancies, electrons, and their pairs are homogeneously distributed so that diffusive flux is minimal. In this limit, we need to consider

$\phi_{i=+, -, \pm}(\mathbf{r}, t) \equiv \phi_i^h(t)$, which satisfy [see Eqs. (33) and (34)]

$$\frac{\partial \phi_+^h(t)}{\partial t} = -\frac{1}{\rho_{+o}} S_{NL}^h(t), \quad (35)$$

$$\frac{\partial \phi_-^h(t)}{\partial t} = -\frac{z_+}{\rho_{-o}} S_{NL}^h(t). \quad (36)$$

Now, consider a case where $\frac{1}{\rho_{\pm o}} = \frac{1}{\rho_{+o}} + \frac{z_+}{\rho_{-o}}$ so that $\phi_+^h(t) + \phi_-^h(t) + \phi_\pm^h(t) = 1$ is satisfied for the nonzero reaction rate $S_{NL}(\mathbf{r}, t) \equiv S_{NL}^h(t)$, given by [see Eq. (31)]

$$S_{NL}^h(t) = K_0(t) \left\{ \exp \left[\frac{\mu_+^h(t)}{\rho_{+o} k_B T} + z_+ \frac{\mu_-^h(t)}{\rho_{-o} k_B T} \right] - \exp \left[\frac{\mu_\pm^h(t)}{\rho_{\pm o} k_B T} \right] \right\}, \quad (37)$$

where we have defined $K_0(t) = \frac{k_B T}{\omega^h(t)} \exp[\frac{p^h(t)}{\rho_{\pm o} k_B T}]$ and used the notation $\omega(\mathbf{r}, t) \equiv \omega^h(t)$, $p(\mathbf{r}, t) \equiv p^h(t)$, $\mu_+(\mathbf{r}, t) \equiv \mu_+^h(t)$, $\mu_-(\mathbf{r}, t) \equiv \mu_-^h(t)$, and $\mu_\pm(\mathbf{r}, t) \equiv \mu_\pm^h(t)$. From Eq. (17), we get

$$\frac{\mu_+^h(t)}{\rho_{+o} k_B T} = \ln \phi_+^h(t) + \frac{G_{+0} + z_+ e \psi^h(t)}{k_B T} - \frac{w_{ij}^v \sigma_{ij}^h(t)}{k_B T}, \quad (38)$$

$$\frac{\mu_-^h(t)}{\rho_{-o} k_B T} = \ln \phi_-^h(t) + \frac{G_{-0} - e \psi^h(t)}{k_B T}, \quad (39)$$

$$\frac{\mu_\pm^h(t)}{\rho_{\pm o} k_B T} = \ln \phi_\pm^h(t) + \frac{G_{\pm 0}}{k_B T}, \quad (40)$$

where $\sigma_{ij}(\mathbf{r}, t) \equiv \sigma_{ij}^h(t)$ and $\psi(\mathbf{r}, t) \equiv \psi^h(t)$. Using Eqs. (38)–(40), we can write Eq. (37) as

$$S_{NL}^h(t) = K_A(t)\phi_+^h(t)[\phi_-^h(t)]^{z_+} - K_D(t)\phi_\pm^h(t), \quad (41)$$

$$K_A(t) = K_0(t) \exp \left[\frac{G_{+0} + z_+ G_{-0}}{k_B T} - \frac{w_{ij}^v \sigma_{ij}^h(t)}{k_B T} \right], \quad (42)$$

$$K_D(t) = K_0(t) \exp \left[\frac{G_{\pm 0}}{k_B T} \right], \quad (43)$$

where $K_A(t)$ and $K_D(t)$ are defined as the time-dependent association and dissociation constants, respectively. It should be noted that the reaction rate $S_{NL}^h(t)$ is independent of the electrostatic potential due to the assumption of a uniform potential. In general, small variations of the electrostatic potential will lead to the dependence of the reaction rate on the potential. Furthermore, the reaction rate depends on the stress due to Vegard's law.

Now, we consider the case of oxygen vacancies so that $z_+ = 2$ and assume that $K_A(t) \equiv K_{A0}$ and $K_D(t) \equiv K_{D0}$. In this case, we can solve Eqs. (35), (36), and (41) in terms of a time-dependent parameter $\alpha(t)$ so that $\phi_+^h(t) = \alpha(t)/\rho_{+0}$, $\phi_-^h(t) = z_+\alpha(t)/\rho_{-0}$ and $\phi_\pm^h(t) = 1 - (1/\rho_{+0} + z_+/\rho_{-0})\alpha(t)$, where $\alpha(t)$ satisfies

$$\begin{aligned} \frac{\partial \alpha(t)}{\partial t} &= -\frac{4K_{A0}}{\rho_{+0}\rho_{-0}^2} \left[\alpha^3(t) + \left(\frac{1}{\rho_{+0}} + \frac{2}{\rho_{-0}} \right) \right. \\ &\quad \times \left. \frac{K_{D0}}{K_{A0}} \frac{\rho_{+0}\rho_{-0}^2}{4} \alpha(t) - \frac{K_{D0}}{K_{A0}} \frac{\rho_{+0}\rho_{-0}^2}{4} \right]. \end{aligned} \quad (44)$$

Although Eq. (44) can be solved exactly, the exact solution obscures identification of a characteristic time. Here, we consider a situation where Eq. (44) can be approximated as

$$\frac{\partial \alpha(t)}{\partial t} = -\frac{4K_{A0}}{\rho_{+0}\rho_{-0}^2} \left[\alpha^3(t) - \frac{K_{D0}}{K_{A0}} \frac{\rho_{+0}\rho_{-0}^2}{4} \right]. \quad (45)$$

Integrating Eq. (45) leads to

$$\begin{aligned} &\ln \left[\frac{\frac{\alpha(t)}{\alpha(\infty)} - 1}{\frac{\alpha(0)}{\alpha(\infty)} - 1} \right]^2 - \ln \left[\frac{\left(\frac{\alpha(t)}{\alpha(\infty)} \right)^2 + \frac{\alpha(t)}{\alpha(\infty)} + 1}{\left(\frac{\alpha(0)}{\alpha(\infty)} \right)^2 + \frac{\alpha(0)}{\alpha(\infty)} + 1} \right] \\ &= -\frac{t}{\tau_0} + 2\sqrt{3} \arctan \left[\frac{1}{\sqrt{3}} + \frac{2}{\sqrt{3}} \frac{\alpha(t)}{\alpha(\infty)} \right] \\ &\quad - 2\sqrt{3} \arctan \left[\frac{1}{\sqrt{3}} + \frac{2}{\sqrt{3}} \frac{\alpha(0)}{\alpha(\infty)} \right], \end{aligned} \quad (46)$$

where τ_0 is the characteristic time of the dissociation of a divalent oxygen vacancy-electron pair and is given by

$$\tau_0 = \frac{\rho_{+0}\rho_{-0}^2}{24K_{A0}\alpha^2(\infty)} = \frac{1}{6} \left[\frac{\rho_{+0}\rho_{-0}^2}{4} \right]^{1/3} \frac{1}{K_{A0}^{1/3} K_{D0}^{2/3}}. \quad (47)$$

The solution of Eq. (46) is plotted in Fig. 1 for different values of the parameter $\alpha(0)/\alpha(\infty)$. Due to the definitions $\phi_+^h(t) = \alpha(t)/\rho_{+0}$, $\phi_-^h(t) = z_+\alpha(t)/\rho_{-0}$, and $\phi_\pm^h(t) = 1 - (1/\rho_{+0} + z_+/\rho_{-0})\alpha(t)$, Fig. 1 reveals an increase in the volume fraction of the vacancies and the electrons resulting

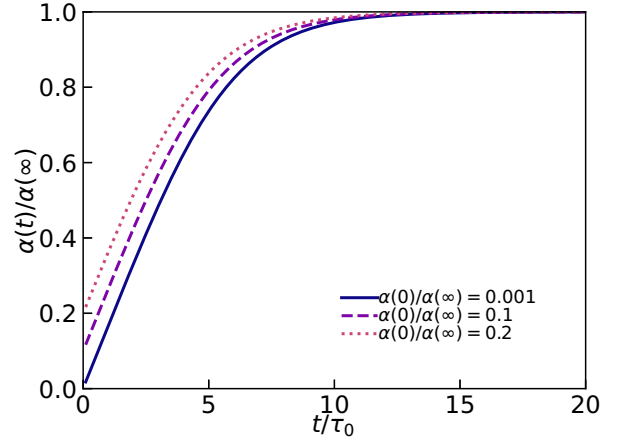


FIG. 1. The solution of Eq. (46) is shown here for different initial conditions.

from the dissociation of vacancy-electron pairs. Also, different values of $\alpha(0)/\alpha(\infty)$ characterize the initial volume fractions of the vacancies, electrons, and their pairs. Furthermore, the dissociation of vacancy-electron pairs is almost complete, i.e., $\alpha(t)/\alpha(\infty) \rightarrow 1$ for $t/\tau_0 > 10$. This implies that the model developed here can be simplified to some extent by considering only dissociated vacancies and electrons for capturing kinetic effects at times much greater than τ_0 . For example, the construction of a polarization-electrostatic potential loop can be done without considering the vacancy-electron pairs at timescales much greater than τ_0 .

B. Steady-state analysis: Implications of Vegard's law

The spatiotemporal responses of oxygen vacancies and electrons to the electrostatic potential and the strain encoded in Eqs. (33) and (34) are asymmetric due to the fact that $z_+ = 2$ and the use of Vegard's law, so only the vacancies affect the strain. In order to make this clearer, the functional derivatives (exchange chemical potentials) appearing in Eqs. (33) and (34) are evaluated as

$$\begin{aligned} &\left[\frac{\mu_+(\mathbf{r}, t)}{k_B T} - \frac{\mu_\pm(\mathbf{r}, t)}{k_B T} \right] \\ &= \ln \left(\frac{\phi_+(\mathbf{r}, t)}{1 - \phi_+(\mathbf{r}, t) - \phi_-(\mathbf{r}, t)} \right) + \frac{z_+ e \psi(\mathbf{r}, t)}{k_B T} \\ &\quad + \frac{G_{+0} - G_{\pm 0}}{k_B T} - \frac{w_{ij}^v \sigma_{ij}(\mathbf{r}, t)}{k_B T} - \frac{\kappa_+ \rho_{+0}}{k_B T} \nabla^2 \phi_+(\mathbf{r}, t) \\ &\quad - \frac{\kappa_{\pm 0} \rho_{\pm 0}}{k_B T} \nabla^2 [\phi_+(\mathbf{r}, t) + \phi_-(\mathbf{r}, t)], \end{aligned} \quad (48)$$

$$\begin{aligned} &\left[\frac{\mu_-(\mathbf{r}, t)}{k_B T} - \frac{\mu_\pm(\mathbf{r}, t)}{k_B T} \right] \\ &= \ln \left(\frac{\phi_-(\mathbf{r}, t)}{1 - \phi_+(\mathbf{r}, t) - \phi_-(\mathbf{r}, t)} \right) - \frac{e \psi(\mathbf{r}, t)}{k_B T} \\ &\quad + \frac{G_{-0} - G_{\pm 0}}{k_B T} - \frac{\kappa_+ \rho_{+0}}{k_B T} \nabla^2 \phi_+(\mathbf{r}, t) \\ &\quad - \frac{\kappa_{\pm 0} \rho_{\pm 0}}{k_B T} \nabla^2 [\phi_+(\mathbf{r}, t) + \phi_-(\mathbf{r}, t)]. \end{aligned} \quad (49)$$

Note that here, the local stress-dependent term appears only in Eq. (48) and results from our assumption that the vacancies affect the local strain, which appears in Eq. (19). Here, we show that the local polarization depends on the spatial distribution of the vacancies and electrons via the electrostatic potential and does not depend solely on the electric field as in classical ferroelectrics. First, we consider the local equilibrium, which corresponds to a steady state of the time-dependent equations. The local equilibrium is defined as the conditions $[\frac{\mu_+(\mathbf{r},t)}{k_B T} - \frac{\mu_-(\mathbf{r},t)}{k_B T}] = 0$ and $[\frac{\mu_-(\mathbf{r},t)}{k_B T} - \frac{\mu_+(\mathbf{r},t)}{k_B T}] = 0$.

At steady state and representing local equilibrium, $\mathbf{P}^*(\mathbf{r}, t) = 0$ and $p = \text{const}$, and hence, $\nabla \cdot \sigma(\mathbf{r}, t) = 0$. Representing all of the variables (independent of time t at $t \rightarrow \infty$) in the steady state by subscript s , we get $\sigma_{ij}(\mathbf{r}, t) \equiv \sigma_{ij,s}(\mathbf{r}) = 0$, where the latter equality represents equilibrium (i.e., a stress-free state). This, in turn, implies that $\epsilon_{ij}(\mathbf{r}, t) \equiv \epsilon_{ij,s}(\mathbf{r}) = \epsilon_{ij,s}^0(\mathbf{r}) = Q_{ijkl} P_{k,s}(\mathbf{r}) P_{l,s}(\mathbf{r}) + w_{ij}^v \rho_{+o} \phi_{+,s}(\mathbf{r})$. For a weakly inhomogeneous distribution of the vacancies and the electrons such that the derivative terms in Eqs. (48) and (49) can be ignored, $[\frac{\mu_+(\mathbf{r},t)}{k_B T} - \frac{\mu_-(\mathbf{r},t)}{k_B T}] = 0$ and $[\frac{\mu_-(\mathbf{r},t)}{k_B T} - \frac{\mu_+(\mathbf{r},t)}{k_B T}] = 0$ lead to

$$\phi_{+,s}(\mathbf{r}) = \frac{1}{1 + \exp \left[\frac{e z_+ \psi_s(\mathbf{r}) - w_{ij}^v \sigma_{ij,s}(\mathbf{r})}{k_B T} + \frac{G_{+o} - G_{\pm o}}{k_B T} \right] \{1 + \exp \left[\frac{e [\psi_s(\mathbf{r}) - \{G_{-o} - G_{\pm o}\}]}{k_B T} \right]\}}, \quad (50)$$

$$\phi_{-,s}(\mathbf{r}) = \frac{1}{1 + \exp \left[- \frac{e [\psi_s(\mathbf{r}) - \{G_{-o} - G_{\pm o}\}]}{k_B T} \right] \{1 + \exp \left[- \frac{e z_+ \psi_s(\mathbf{r}) - w_{ij}^v \sigma_{ij,s}(\mathbf{r})}{k_B T} - \frac{G_{+o} - G_{\pm o}}{k_B T} \right]\}}, \quad (51)$$

where we have used the notation $\psi(\mathbf{r}, t \rightarrow \infty) = \psi_s(\mathbf{r})$ and $\sigma_{ij}(\mathbf{r}, t \rightarrow \infty) = \sigma_{ij,s}(\mathbf{r})$. Using these equations, it is clear that the effects of vacancies on the total strain appear via the Vegard strain and lead to the result (valid at the steady state)

$$\epsilon_{ij,s}(\mathbf{r}) = Q_{ijkl} P_{k,s}(\mathbf{r}) P_{l,s}(\mathbf{r}) + \frac{w_{ij}^v \rho_{+o}}{1 + \exp \left[\frac{e z_+ \psi_s(\mathbf{r}) - w_{ij}^v \sigma_{ij,s}(\mathbf{r})}{k_B T} + \frac{G_{+o} - G_{\pm o}}{k_B T} \right] \{1 + \exp \left[\frac{e [\psi_s(\mathbf{r}) - \{G_{-o} - G_{\pm o}\}]}{k_B T} \right]\}}. \quad (52)$$

A similar result without any consideration of the self-energy terms (i.e., without G_{lo}) was derived in Ref. [6]. In Fig. 2, we plot the Vegard strain as a function of the electrostatic potential [see Eq. (52)] for different values the self-energies of the divalent vacancies and electrons in a stress-free state [i.e., $\sigma_{ij,s}(\mathbf{r}) = 0$]. In order to highlight the effects of the electrostatic potential on the Vegard strain, we plot only the second term on the right-hand side of Eq. (52); i.e., $Q_{ijkl} P_{k,s}(\mathbf{r}) P_{l,s}(\mathbf{r})$ is not considered. Furthermore, Eq. (52) is plotted by varying

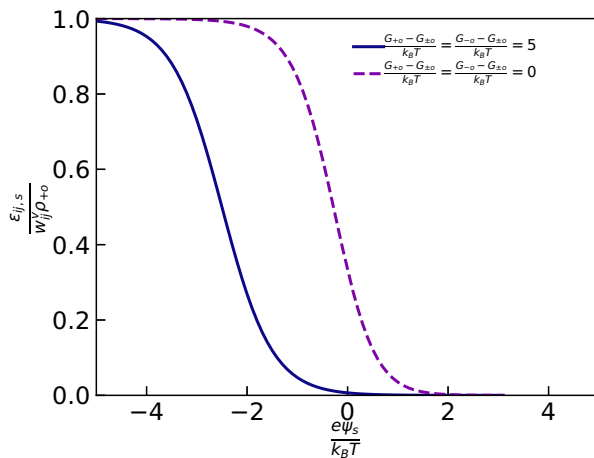


FIG. 2. The Vegard strain given by Eq. (52) is plotted as a function of the electrostatic potential for a stress-free state [i.e., $\sigma_{ij,s}(\mathbf{r}) = 0$] with different values of self-energies of the divalent vacancies (i.e., $z_+ = 2$) and electrons. For simplicity, the self-energies of a vacancy and an electron are assumed to be equal. To highlight the asymmetric effects of the electrostatic potential on the Vegard strain, we plot only the second term on the right-hand side of Eq. (52); i.e., $Q_{ijkl} P_{k,s}(\mathbf{r}) P_{l,s}(\mathbf{r})$ is not plotted.

the electrostatic potential at a given location such as the surface of a ferroelectric film probed using piezoresponse force microscopy. Figure 2 shows that the Vegard strain depends in an asymmetric manner on the electrostatic potential and the asymmetry increases with an increase in the magnitude of the self-energies. This implies that if the surface potential is changed in a systematic manner, then the strain-electrostatic potential loop will be asymmetric with respect to the sign of the electrostatic potential, in qualitative agreement with the experiments [6].

Additionally, the vacancies affect the local electric field. At the local equilibrium, $\mathbf{P}_s(\mathbf{r}) = \alpha(\mathbf{r}) \mathbf{E}(\mathbf{r})$, where the prefactor $\alpha(\mathbf{r})$ depends on the specific form of H and can be determined numerically for any functional form of H . $\mathbf{E}(\mathbf{r}) = \mathbf{E}_0(\mathbf{r}) + \mathbf{E}_1(\mathbf{r})$, where $\nabla \cdot \{\epsilon_0 \epsilon_\infty + \alpha(\mathbf{r})\} \mathbf{E}_0(\mathbf{r}) = 0$ and $\nabla \cdot \{\epsilon_0 \epsilon_\infty + \alpha(\mathbf{r})\} \mathbf{E}_1(\mathbf{r}) = e z_+ \rho_{+o} \phi_{+,s}(\mathbf{r}) - e \rho_{-o} \phi_{-,s}(\mathbf{r})$. In other words, the local electric field has a contribution \mathbf{E}_1 resulting from inhomogeneous distribution of vacancies and oppositely charged carriers. It should be noted that $\mathbf{E}_1 = \mathbf{E}_0$ in the absence of vacancies but $\mathbf{E}_1 \neq \mathbf{E}_0$ in the presence of charged vacancies. This, in turn, implies that the local polarization $\mathbf{P}_s(\mathbf{r}) = \alpha(\mathbf{r}) [\mathbf{E}_0(\mathbf{r}) + \mathbf{E}_1(\mathbf{r})]$ is intimately connected to the spatial distribution of vacancies and electrons.

C. Coupling between the fast and slow components of the polarization: Topological effects in the vacancy-free regime

The model developed here is based on the decomposition of the net local polarization into a slowly varying component, \mathbf{P} , and a fast component, \mathbf{P}_e . Coupling between these two components appears in the form of ϵ_∞ in the model, which affects the electrostatic potential $\psi(\mathbf{r}, t)$. In addition,

another coupling appears in Eq. (25) in the form of the lattice velocity \mathbf{v}_l , which can be interpreted in terms of the rate of the change of the net local polarization. The molecular origin of this interpretation is the fact that the local displacement of electrons and ions of ferroelectric crystals contributes to the net polarization, which is treated in the model as \mathbf{P}_e and \mathbf{P} , respectively. This, in turn, leads to the relation $\mathbf{v}_l(\mathbf{r}, t) \sim \partial[\mathbf{P}_e(\mathbf{r}, t) + \mathbf{P}(\mathbf{r}, t)]/\partial t$. In most of the phase field

models, $\mathbf{v}_l(\mathbf{r}, t)$ is taken to be zero, which implies that $\mathbf{v}_l(\mathbf{r}, t) \simeq \partial[\mathbf{P}_e(\mathbf{r}, t)]/\partial t \rightarrow 0$ at the timescales relevant to the models. This implies that Eq. (25) can be written as

$$\frac{\partial \mathbf{P}(\mathbf{r}, t)}{\partial t} = \mathbf{P}^*(\mathbf{r}, t), \quad (53)$$

where Eqs. (17) and (25) allow us to identify

$$\mathbf{P}^*(\mathbf{r}, t) = -\frac{1}{\tau_p} \left[\frac{\delta[\int d\mathbf{r}' H_{\text{LGD}}\{\mathbf{P}(\mathbf{r}', t)\} + H_{\text{grad}}\{\nabla \mathbf{P}(\mathbf{r}', t)\}]}{\delta \mathbf{P}(\mathbf{r}, t)} - \mathbf{E}(\mathbf{r}, t) \right]. \quad (54)$$

In general, $H_{\text{LGD}} + H_{\text{grad}}$ can be written in powers of \mathbf{P} so that

$$H_{\text{LGD}}\{\mathbf{P}\} + H_{\text{grad}}\{\nabla \mathbf{P}\} = \frac{1}{2\chi} \mathbf{P}^2(\mathbf{r}, t) + \frac{\kappa_{p,1}}{2} [\nabla \cdot \mathbf{P}(\mathbf{r}, t)]^2 + \frac{\kappa_{p,2}}{2} [\nabla \times \mathbf{P}(\mathbf{r}, t)]^2 + \kappa_{p,3} \mathbf{P}(\mathbf{r}, t) \cdot [\nabla \times \mathbf{P}(\mathbf{r}, t)]. \quad (55)$$

Equations (54) and (55) lead to

$$\mathbf{P}^*(\mathbf{r}, t) = -\frac{1}{\tau_p} \left\{ \frac{1}{\chi} \mathbf{P}(\mathbf{r}, t) - \kappa_{p,1} \nabla [\nabla \cdot \mathbf{P}(\mathbf{r}, t)] + \kappa_{p,2} \nabla \times [\nabla \times \mathbf{P}(\mathbf{r}, t)] + 2\kappa_{p,3} [\nabla \times \mathbf{P}(\mathbf{r}, t)] - \mathbf{E}(\mathbf{r}, t) \right\}. \quad (56)$$

Using Eq. (23) in the absence of the vacancies and electrons and $\nabla \times \mathbf{E}(\mathbf{r}, t) = 0$,

$$\nabla \cdot \mathbf{P}^*(\mathbf{r}, t) = -\frac{1}{\tau_p} \left[\left\{ \frac{1}{\chi} + \frac{1}{\epsilon_0 \epsilon_\infty} \right\} \nabla \cdot \mathbf{P}(\mathbf{r}, t) - \kappa_{p,1} \nabla^2 [\nabla \cdot \mathbf{P}(\mathbf{r}, t)] \right], \quad (57)$$

$$\nabla \times \mathbf{P}^*(\mathbf{r}, t) = -\frac{1}{\tau_p} \left[\frac{1}{\chi} \nabla \times \mathbf{P}(\mathbf{r}, t) + \kappa_{p,2} \nabla \times \{ \nabla \times [\nabla \times \mathbf{P}(\mathbf{r}, t)] \} + 2\kappa_{p,3} \nabla \times [\nabla \times \mathbf{P}(\mathbf{r}, t)] \right]. \quad (58)$$

Operating with divergence and curl in Eq. (53) and using Eqs. (57) and (58), we get

$$\frac{\partial [\nabla \cdot \mathbf{P}(\mathbf{r}, t)]}{\partial t} = \left[\frac{\kappa_{p,1}}{\tau_p} \nabla^2 - \frac{1}{\tau_L} \right] [\nabla \cdot \mathbf{P}(\mathbf{r}, t)], \quad (59)$$

$$\frac{\partial [\nabla \times \mathbf{P}(\mathbf{r}, t)]}{\partial t} = \left[\frac{\kappa_{p,2}}{\tau_p} \nabla^2 - \frac{2\kappa_{p,3}}{\tau_p} (\nabla \times) - \frac{1}{\tau_p \chi} \right] [\nabla \times \mathbf{P}(\mathbf{r}, t)], \quad (60)$$

where $\tau_L = \tau_p / \{ \frac{1}{\chi} + \frac{1}{\epsilon_0 \epsilon_\infty} \}$ is the characteristic time for the change in $\nabla \cdot \mathbf{P}(\mathbf{r}, t)$ and $\tau_p \chi$ is the characteristic time for the change in $\nabla \times \mathbf{P}(\mathbf{r}, t)$. Note that $\tau_L / (\tau_p \chi) = 1 / [1 + \chi / (\epsilon_0 \epsilon_\infty)] \ll 1$ for $\chi \gg 1$. This means that for $t \gg \tau_L$, $\nabla \cdot \mathbf{P}(\mathbf{r}, t) = 0$. This allows us to identify the relation between the local polarization and the electric field by using Eq. (53). For example, in a steady state, $\mathbf{P}^*(\mathbf{r}, t) = 0$, which leads to the following relation between the local polarization and the local electric field:

$$\begin{aligned} \frac{1}{\chi} \mathbf{P}_s(\mathbf{r}) - \kappa_{p,1} \nabla [\nabla \cdot \mathbf{P}_s(\mathbf{r})] + \kappa_{p,2} \nabla \\ \times [\nabla \times \mathbf{P}_s(\mathbf{r})] + 2\kappa_{p,3} [\nabla \times \mathbf{P}_s(\mathbf{r})] = \mathbf{E}_s(\mathbf{r}), \end{aligned} \quad (61)$$

where we have used the notation $\mathbf{P}_s(\mathbf{r}) = \mathbf{P}(\mathbf{r}, \infty)$ and $\mathbf{E}_s(\mathbf{r}) = \mathbf{E}(\mathbf{r}, \infty)$. For a given volume, the solution of Eq. (61) depends on the geometry and boundary conditions. A particular set of solutions which enforces $\nabla \cdot \mathbf{P}_s(\mathbf{r}) = 0$ everywhere in space including the boundaries will be discussed here. In particular, $\nabla \times \mathbf{P}_s(\mathbf{r}) = \lambda \mathbf{P}_s(\mathbf{r})$, which enforces $\nabla \cdot \mathbf{P}_s(\mathbf{r}) = 0$ for a constant λ will be discussed here. For such a

divergence-free polarization vector, Eq. (61) demands

$$\left[\frac{1}{\chi} + \kappa_{p,2} \lambda^2 + 2\kappa_{p,3} \lambda \right] \mathbf{P}_s(\mathbf{r}) = \mathbf{E}_s(\mathbf{r}). \quad (62)$$

Equation (62) shows that $\mathbf{P}_s(\mathbf{r})$ and $\mathbf{E}_s(\mathbf{r})$ are parallel to each other in the steady state, which may not be true in general. The nonzero solutions of $\nabla \times \mathbf{P}_s(\mathbf{r}) = \lambda \mathbf{P}_s(\mathbf{r})$ are called Beltrami [38] fields and have been studied extensively [39] in fluid mechanics [40] and magnetodynamics [41,42]. These solutions depend on geometry and symmetry and are quantized in certain cases. As an example, for a spherical volume of radius R , a nontrivial solution of $\nabla \times \mathbf{P}_s(\mathbf{r}) = \lambda \mathbf{P}_s(\mathbf{r})$ so that $\mathbf{P}_s(\mathbf{r}) \cdot \hat{\mathbf{r}} = 0$ at the boundary ($\hat{\mathbf{r}}$ is a unit vector along the radial direction) can be written as [43,44]

$$\mathbf{P}_s(\mathbf{r}) = u(r, \theta) \hat{\mathbf{r}} + v(r, \theta) \hat{\theta} + w(r, \theta) \hat{\phi}, \quad (63)$$

$$u(r, \theta) = \frac{2}{\lambda^2 r^2} \left[\frac{\sin \lambda r}{\lambda r} - \cos \lambda r \right] \cos \theta, \quad (64)$$

$$v(r, \theta) = -\frac{1}{\lambda r} \left[\cos \lambda r - \frac{\sin \lambda r}{\lambda r} + \lambda r \sin \lambda r \right] \sin \theta, \quad (65)$$

$$w(r, \theta) = \frac{1}{\lambda r} \left[\frac{\sin \lambda r}{\lambda r} - \cos \lambda r \right] \sin \theta. \quad (66)$$

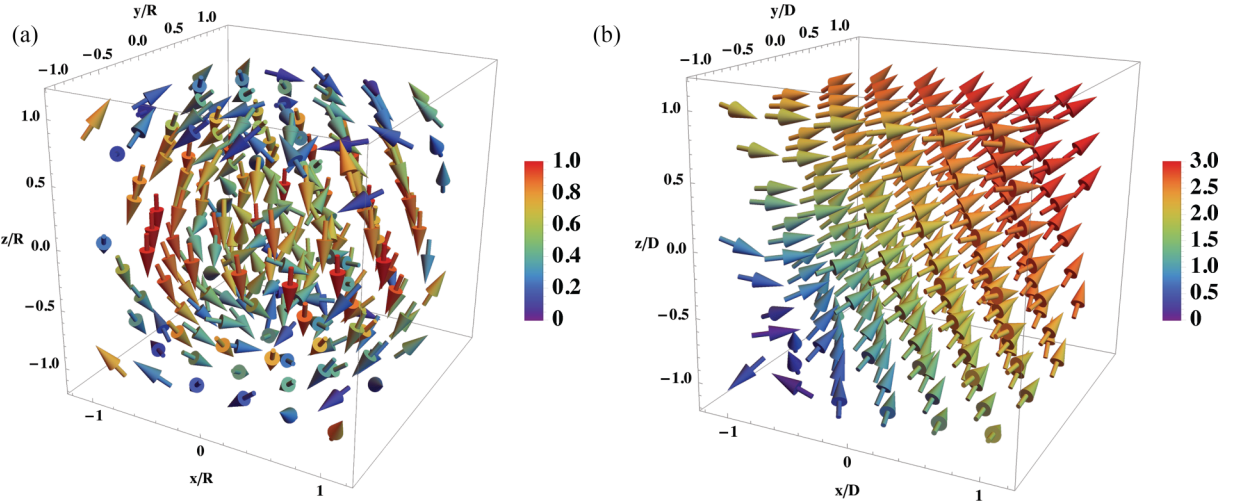


FIG. 3. Solutions of the Beltrami equation $\nabla \times \mathbf{P}_s(\mathbf{r}) = \lambda \mathbf{P}_s(\mathbf{r})$ are shown. (a) $\mathbf{P}_s(\mathbf{r})$ inside a sphere of radius R described using Eq. (63) with the boundary condition $\mathbf{P}_s(\mathbf{r}) \cdot \hat{\mathbf{f}} = 0$. Conversion from polar spherical coordinates to Cartesian coordinates is done to plot $\mathbf{P}_s(\mathbf{r})$. (b) Solution of the Beltrami equation with periodic boundary conditions described by Eq. (67). (b) is for $A = B = C = 1$. Also, $\lambda = 4.4934/R$, and $\lambda = 1/D$ for (a) and (b), respectively.

Here, $\lambda = 4.4934/R$ leads to a nontrivial solution of $\nabla \times \mathbf{P}_s(\mathbf{r}) = \lambda \mathbf{P}_s(\mathbf{r})$ with the lowest helicity, where the helicity of the vector field $\mathbf{P}_s(\mathbf{r})$ is $\int d\mathbf{r} \mathbf{P}_s(\mathbf{r}) \cdot \nabla \times \mathbf{P}_s(\mathbf{r}) = \lambda \int d\mathbf{r} \mathbf{P}_s(\mathbf{r}) \cdot \mathbf{P}_s(\mathbf{r}) = 25.25$, which is independent of R . Equation (63) is plotted in Fig. 3(a) and requires the existence of an electric field, which satisfies Eq. (62) with $\lambda = 4.4934/R$. Furthermore, there are solutions of $\nabla \times \mathbf{P}_s(\mathbf{r}) = \lambda \mathbf{P}_s(\mathbf{r})$ which satisfy periodic boundary conditions [38,40]. For example, for $\lambda = 1/D$,

$$\mathbf{P}_s(\mathbf{r}) = u(y, z)\hat{x} + v(x, z)\hat{y} + w(x, y)\hat{z}, \quad (67)$$

$$u(y, z) = A \sin \frac{z}{D} + C \cos \frac{y}{D}, \quad (68)$$

$$v(x, z) = B \sin \frac{x}{D} + A \cos \frac{z}{D}, \quad (69)$$

$$w(x, y) = C \sin \frac{y}{D} + B \cos \frac{x}{D}. \quad (70)$$

Equation (67) is plotted in Fig. 3(b), and like in the spherical geometry, the existence of such a topological configuration requires the existence of an electric field, which satisfies Eq. (62) with $\lambda = 1/D$. Similar to the steady-state analysis presented here, Eq. (53) can be used to determine the time-dependent electric field required for setting up a known polarization vector in space and time.

In contrast to the above analysis, if we consider $\mathbf{v}_l(\mathbf{r}, t) = \beta \partial \mathbf{P}(\mathbf{r}, t) / \partial t$, where β is a constant, then Eq. (25) can be written as

$$\begin{aligned} \frac{\partial \mathbf{P}(\mathbf{r}, t)}{\partial t} + \beta \left[\frac{\partial \mathbf{P}(\mathbf{r}, t)}{\partial t} \cdot \nabla \right] \mathbf{P}(\mathbf{r}, t) + \frac{\beta}{2} \mathbf{P}(\mathbf{r}, t) \\ \times \frac{\partial [\nabla \times \mathbf{P}(\mathbf{r}, t)]}{\partial t} = \mathbf{P}^*(\mathbf{r}, t). \end{aligned} \quad (71)$$

Equation (71) shows that the coupling between the slow and fast components of the net polarization will affect the spatiotemporal distribution of $\mathbf{P}(\mathbf{r}, t)$, while the steady-state behavior of $\mathbf{P}(\mathbf{r}, t) \equiv \mathbf{P}_s(\mathbf{r})$ remains the same. Equation (71) opens up a way to study the effects of

confinement on the spatiotemporal distribution of topologically nontrivial polarization, which may not be realized at equilibrium.

IV. CONCLUSIONS

We developed a thermodynamically consistent time-dependent model for understanding the effects of multivalent vacancies on relations between the polarization-electric potential and strain-electric potential in thin films of ferroelectrics. In contrast to most of the phase field models, nonlinear effects of the reaction kinetics leading to the generation of charged vacancies and electrons from their pairs are introduced in the model. In addition, the diffusion and elastic effects of the charged vacancies were considered, which were shown to exhibit asymmetric responses of the strain to the electric potential. Furthermore, the model introduced coupling between the slow component and a fast component of the net polarization, which is expected to affect the time-dependent relation between the polarization and the electric field. The impedance response of thin films of ferroelectrics with vacancies should exhibit an electrode polarization phenomenon [20] due to localization of the vacancies near an oppositely charged electrode. The electrode polarization phenomenon can be used to extract the diffusion constant of the vacancies. A simplified model [20] developed using the Rayleighian approach was used previously to fit the impedance spectra as a function of frequency and temperature for thin films of ionic polymers. We envision that in the future, the experimental results for impedance spectra from thin films of ferroelectrics with vacancies will be able to be fitted using the model developed here and will be able to extract the diffusion constant of the vacancies. The Rayleighian approach to build the model was shown to be general enough for constructing nonlinear reaction kinetics. Application of the model to simulate the motion of domain walls in ferroelectrics in the presence of vacancies will be presented in a future publication.

ACKNOWLEDGMENTS

This work was supported by the Center for Nanophase Materials Sciences, which is a U.S. DOE, Office of Science User Facility at Oak Ridge National Laboratory. ORNL is managed by UT-Battelle, LLC, under Contract No. DE-AC05-00OR22725 for the U.S. Department of Energy. The U.S. Government is authorized to reproduce and distribute reprints for Government purposes notwithstanding any

copyright notation hereon. The Department of Energy will provide public access to these results of federally sponsored research in accordance with the DOE Public Access Plan [45].

DATA AVAILABILITY

The data that support the findings of this study are available from the corresponding author upon reasonable request.

-
- [1] M. Imada, A. Fujimori, and Y. Tokura, Metal-insulator transitions, *Rev. Mod. Phys.* **70**, 1039 (1998).
 - [2] D. D. Awschalom and M. E. Flatté, Challenges for semiconductor spintronics, *Nat. Phys.* **3**, 153 (2007).
 - [3] K. M. Rabe, M. Dawber, C. Lichtensteiger, C. H. Ahn, and J.-M. Triscone, Modern physics of ferroelectrics: Essential background, in *Physics of Ferroelectrics: A Modern Perspective* (Springer-Verlag, Berlin, Heidelberg, 2007), pp. 1–30.
 - [4] S. Oh, H. Hwang, and I. K. Yoo, Ferroelectric materials for neuromorphic computing, *APL Mater.* **7**, 091109 (2019).
 - [5] J. Jeong, N. Aetukuri, T. Graf, T. D. Schladt, M. G. Samant, and S. S. P. Parkin, Suppression of metal-insulator transition in VO₂ by electric field induced oxygen vacancy formation, *Science* **339**, 1402 (2013).
 - [6] K. P. Kelley, A. N. Morozovska, E. A. Eliseev, V. Sharma, D. E. Yilmaz, A. C. T. van Duin, P. Ganesh, A. Borisevich, S. Jesse, P. Maksymovych *et al.*, Oxygen vacancy injection as a pathway to enhancing electromechanical response in ferroelectrics, *Adv. Mater.* **34**, 2106426 (2022).
 - [7] S. M. Yang, A. N. Morozovska, R. Kumar, E. A. Eliseev, Y. Cao, L. Mazet, N. Balke, S. Jesse, R. K. Vasudevan, C. Dubourdieu *et al.*, Mixed electrochemical–ferroelectric states in nanoscale ferroelectrics, *Nat. Phys.* **13**, 812 (2017).
 - [8] D. Akbarian, D. E. Yilmaz, Y. Cao, P. Ganesh, I. Dabo, J. Munro, R. Van Ginneken, and A. C. T. Van Duin, Understanding the influence of defects and surface chemistry on ferroelectric switching: A ReaxFF investigation of BaTiO₃, *Phys. Chem. Chem. Phys.* **21**, 18240 (2019).
 - [9] Y. Xiao and K. Bhattacharya, A continuum theory of deformable, semiconducting ferroelectrics, *Arch. Ration. Mech. Anal.* **189**, 59 (2008).
 - [10] J. L. Lin, R. He, Z. Lu, Y. Lu, Z. Wang, Z. Zhong, X. Zhao, R.-W. Li, Z. D. Zhang, and Z. J. Wang, Oxygen vacancy enhanced ferroelectricity in BTO:SRO nanocomposite films, *Acta Mater.* **199**, 9 (2020).
 - [11] Y. L. Li, S. Y. Hu, Z. K. Liu, and L. Q. Chen, Phase-field model of domain structures in ferroelectric thin films, *Appl. Phys. Lett.* **78**, 3878 (2001).
 - [12] A. K. Saha, K. Ni, Sourav Dutta, Suman Datta, and S. Gupta, Phase field modeling of domain dynamics and polarization accumulation in ferroelectric HZO, *Appl. Phys. Lett.* **114**, 202903 (2019).
 - [13] J.-J. Wang, B. Wang, and L.-Q. Chen, Understanding, predicting, and designing ferroelectric domain structures and switching guided by the phase-field method, *Annu. Rev. Mater. Res.* **49**, 127 (2019).
 - [14] L.-Q. Chen, Appendix A–Landau free-energy coefficients, in *Physics of Ferroelectrics: A Modern Perspective* (Springer-Verlag, Berlin, Heidelberg, 2007), pp. 363–372.
 - [15] Y. Zhang, J. Li, and D. Fang, Oxygen-vacancy-induced memory effect and large recoverable strain in a barium titanate single crystal, *Phys. Rev. B* **82**, 064103 (2010).
 - [16] Y. Cao, J. Shen, C. Randall, and L.-Q. Chen, Effect of ferroelectric polarization on ionic transport and resistance degradation in BaTiO₃ by phase-field approach, *J. Am. Ceram. Soc.* **97**, 3568 (2014).
 - [17] Y. Shindo, F. Narita, and T. Kobayashi, Phase field simulation on the electromechanical response of poled barium titanate polycrystals with oxygen vacancies, *J. Appl. Phys.* **117**, 234103 (2015).
 - [18] P. Fedeli, M. Kamlah, and A. Frangi, Phase-field modeling of domain evolution in ferroelectric materials in the presence of defects, *Smart Mater. Struct.* **28**, 035021 (2019).
 - [19] R. A. Marcus, Electrostatic free energy and other properties of states having nonequilibrium polarization. I, *J. Chem. Phys.* **24**, 979 (1956).
 - [20] R. Kumar, J. P. Mahalik, V. Bocharova, E. W. Stacy, C. Gainaru, T. Saito, M. P. Gobet, S. Greenbaum, B. G. Sumpter, and A. P. Sokolov, A Rayleighian approach for modeling kinetics of ionic transport in polymeric media, *J. Chem. Phys.* **146**, 064902 (2017).
 - [21] A. R. Denton and N. W. Ashcroft, Vegard’s law, *Phys. Rev. A* **43**, 3161 (1991).
 - [22] L. Onsager, Reciprocal relations in irreversible processes. I, *Phys. Rev.* **37**, 405 (1931).
 - [23] S. R. Groot and P. Mazur, *Non-equilibrium Thermodynamics*, Dover Books on Physics and Chemistry (Dover Publications, North-Holland, 1962).
 - [24] L. Onsager and S. Machlup, Fluctuations and irreversible processes, *Phys. Rev.* **91**, 1505 (1953).
 - [25] M. Doi, J. Zhou, Y. Di, and X. Xu, Application of the Onsager-Machlup integral in solving dynamic equations in nonequilibrium systems, *Phys. Rev. E* **99**, 063303 (2019).
 - [26] M. Doi, Onsager’s variational principle in soft matter, *J. Phys.: Condens. Matter* **23**, 284118 (2011).
 - [27] J. Cummings, J. S. Lowengrub, B. G. Sumpter, S. M. Wise, and R. Kumar, Modeling solvent evaporation during thin film formation in phase separating polymer mixtures, *Soft Matter* **14**, 1833 (2018).
 - [28] J. Hubbard and L. Onsager, Dielectric dispersion and dielectric friction in electrolyte solutions. I, *J. Chem. Phys.* **67**, 4850 (1977).
 - [29] B. U. Felderhof and H. J. Kroh, Hydrodynamics of magnetic and dielectric fluids in interaction with the electromagnetic field, *J. Chem. Phys.* **110**, 7403 (1999).
 - [30] L. D. Landau, L. P. Pitaevskii, E. M. Lifshitz, and A. M. Kosevich, *Theory of Elasticity*, 3rd ed. (Butterworth-Heinemann, 1986).

- [31] T. Mura, General theory of eigenstrains, in *Micromechanics of Defects in Solids* (Kluwer Academic Publishers, Dordrecht, The Netherlands, 1987), pp. 1–73.
- [32] L.-Q. Chen, Phase-field models for microstructure evolution, *Annu. Rev. Mater. Res.* **32**, 113 (2002).
- [33] J. Israelachvili, *Intermolecular and Surface Forces* (Academic Press, London, 1992).
- [34] R. Kumar, B. G. Sumpter, and M. Muthukumar, Enhanced phase segregation induced by dipolar interactions in polymer blends, *Macromolecules* **47**, 6491 (2014).
- [35] S. Glasstone, K. Laidler, and H. Eyring, *The Theory of Rate Processes* (McGraw-Hill, New York, 1941).
- [36] R. Kumar, Z. Liu, B. Lokitz, J. Chen, J.-M. Carrillo, J. Jakowski, C. P. Collier, S. Retterer, and R. Advincula, Harnessing autocatalytic reactions in polymerization and de-polymerization, *MRS Commun.* **11**, 377 (2021).
- [37] J. Newman and N. P. Balsara, *Electrochemical Systems* (Wiley, Hoboken, NJ, 2021).
- [38] E. Beltrami, Considerazioni idrodinamiche, *Nuovo Cim.* **25**, 212 (1889).
- [39] N. Sato and M. Yamada, Local representation and construction of Beltrami fields, *Physica D (Amsterdam, Netherlands)* **391**, 8 (2019).
- [40] V. I. Arnold and B. A. Khesin, *Topological Methods in Hydrodynamics*, Applied Mathematical Sciences Vol. 125 (Springer, Cham, 2021).
- [41] S. Chandrasekhar and L. Woltjer, On force-free magnetic fields, *Proc. Natl. Acad. Sci. USA* **44**, 285 (1958).
- [42] L. Woltjer, A theorem on force-free magnetic fields, *Proc. Natl. Acad. Sci. USA* **44**, 489 (1958).
- [43] S. Chandrasekhar and P. C. Kendall, On force-free magnetic fields, *Astrophys. J.* **126**, 457 (1957).
- [44] J. Cantarella, D. DeTurck, H. Gluck, and M. Teytel, The spectrum of the curl operator on spherically symmetric domains, *Phys. Plasmas* **7**, 2766 (2000).
- [45] <https://www.energy.gov/doe-public-access-plan>.